

Fabrication and Evaluation of Curcumin-loaded Nanoparticles Based on Solid Lipid as a New Type of Colloidal Drug Delivery System

J. CHEN, W. T. DAI, Z. M. HE, L. GAO, X. HUANG¹, J. M. GONG¹, H. Y. XING AND W. D. CHEN^{*,1}

Department of Pharmacy, The Second People's Hospital of Hefei, Hefei-230 011, ¹College of Pharmacy, The Traditional Chinese Medicine College of Anhui, Hefei-230 031, China

Chen, *et al.*: Curcumin Solid Lipid Nanoparticles

Curcumin has very broad spectrum of biological activities; however, photodegradation, short half-life and low bioavailability have limited its clinical application. Curcumin-loaded solid lipid nanoparticles were studied to overcome these problems. The aim of this study was to optimize the best formulation on curcumin-loaded solid lipid nanoparticles. Emulsion-evaporation and low temperature-solidification technique was applied with monostearin as lipid carriers. The single factor analysis and orthogonal design were used to optimize formulation and various parameters were investigate. By the optimisation of a single factor analysis and orthogonal test, the particles size, polydispersity index, zeta potential, encapsulation efficiency and drug loading capacity of the optimised formulation were 99.99 nm, 0.158, -19.9 mV, 97.86%, and 4.35%, respectively. The differential scanning calorimetry and X-ray diffraction analysis results demonstrated new structure was formed in nanoparticles. The release kinetics *in vitro* demonstrated curcumin-loaded solid lipid nanoparticles can control drug release. These studies confirmed that curcumin-loaded solid lipid nanoparticles could be prepared successfully with high drug entrapment efficiency and loading capacity. Curcumin-loaded solid lipid nanoparticles may be a promising drug delivery system to control drug release and improve bioavailability.

Key words: Curcumin, preparation, release, solid lipid nanoparticles

Solid lipid nanoparticles (SLNs) were developed at the beginning of the 1990s as an alternative colloidal lipidic system for controlled drug delivery. SLNs were made from solid lipid only, which were essentially composed of a biocompatible lipid core with entrapped lipophilic drug and surfactant at the outer shell. The structure of SLNs could be compared with a 'symmetric brick wall'^[1]. SLNs dispersions had been proposed as a new type of colloidal drug carrier system suitable for intravenous administration.

In fact, SLNs were nanometre-sized drug delivery systems, which combined the advantages of polymeric nanoparticles, emulsion, and liposomes. The advantages includes good biocompatibility, protection of the incorporated compound against degradation and controlled release of drug; especially, SLNs

that contained the lipid matrix, which decreased the potential for acute and chronic toxicity.

Curcumin (CUR), which is a bright orange-yellow pigment of turmeric, India's gold obtained from *Curcuma longa* is a household spice in India. The essential component of the turmeric is CUR and curcuminoids. It has very broad spectrum of biological activities such as antiinflammator^[2], antioxidant^[3], antimicrobial^[4], and anticancer^[5,6]. It also has been shown to lower the cholesterol by increasing the low density lipoprotein receptor (LDL-R)^[7]. Chemopreventive and growth inhibitory activities of CUR against many tumour cell lines have been reported^[8,9].

CUR is also a potent scavenger of various reactive oxygen species (ROS) (including reactive oxygen intermediates (ROI) and reactive nitrogen intermediates (RNI)) including superoxide anions and hydroxyl radicals. CUR may help prevent and

***Address for correspondence**

E-mail: anzhongdong@126.com

treat patients with Alzheimer's disease by reducing oxidative damage, plaque burden and suppressing specific inflammatory factors^[10,11]. The ROS has been targeted as 'evil molecules'. In fact, it was the first line of defence against the plethora of intracellular pathogens. CUR is known to increase the phagocytic activity on one hand^[12], and decrease the ROI and RNI^[13,14] on the other hand, thereby raising an alarm.

Although CUR has shown a wide range of pharmacological activities, there were also some potential limitations. Photodegradation, short half-life and low bioavailability were major hurdles for the therapeutic use of CUR^[15]. CUR, with phenolic group and conjugated double bonds, which is unstable in the presence of light and basic pH, degrades within 30 min^[16,17]. In addition, the poor oral bioavailability was due to its low water solubility under acidic or neutral conditions^[18]. Various methods have been tried to overcome these bioavailability problems. The aim of the present study was to formulate SLNs to increase photostability and enhance its anticancer activity because it can not only overcome the membrane stability and drug-leaching, but also reduce the potential toxicity of CUR^[19].

The first aim of this study was to evaluate and optimize the best formulation by a single factor analysis and orthogonal design. Secondly, the physicochemical properties including morphology, particles size (Z-ave), polydispersity index (PDI), zeta potential (ZP), encapsulation efficiency (EE) and drug loading (DL) capacity were characterised. Crystal structure of CUR, excipients, physical mixture and lyophilised curcumin-loaded SLNs (CUR-SLNs) were also investigated. In addition, the release behaviour of curcumin suspension (CUR-suspension) and CUR-SLNs *in vitro* were evaluated to provide research foundation for pharmacokinetics and tissue distribution *in vivo*.

MATERIALS AND METHODS

CUR (>95%) was purchased from Henan Guangye Natural Pigmen Co., Ltd., China. Monostearin (MS) was purchased from Hunan Erkang Pharmaceutical Co., Ltd., China. F68 was obtained from BASF, Germany. T-80 was purchased from Sonopharm Chemical Reagent Co., Ltd., China. Lecithin was provided by Anhui Fengyuan Pharmaceutical Co.,

Ltd., China. Methanol was of high performance liquid chromatography (HPLC) grade. All other reagents and solvents were of analytical grade.

Preparation and lyophilisation of SLNs:

CUR-SLNs were prepared by emulsion-evaporation and low temperature-solidification technique, which was reported by our study previously^[20]. Briefly, the lipid phase and the lipophilic surfactant were dissolved in the right amount of organic solvents and heated up to 75° to obtain a homogeneous solution. Following the addition of CUR, the hot lipid phase was dispersed into the aqueous solution of hydrophilic surfactant, heated at the same temperature, by high speed stirring (1000 rpm) (ETS-D4 stirrer, IKA, Germany) for 2 h to form preemulsion. The resulting hot o/w nanoemulsion was dumped into ice cold distilled water (0°) quickly under mild mechanical for 2 h. CUR-SLNs were formed by lipid recrystallisation. The blank SLNs were prepared by the same procedure without adding CUR. The SLNs formulation was previously optimised by a single factor analysis and orthogonal design.

Mannitol at a concentration of 4% w/w as cryoprotectant was used in the freeze-drying process. The SLNs dispersion were prefrozen using an ultra-cold freezer (MDF-382E, SANYO, Japan) at -80° for 24 h, and then were transferred to the freeze-dryer (LGJ 0.5, Beijing, China) for 72 h. The SLNs powder was collected for further experiment.

Transmission electron microscope:

The morphology of the nanoparticles was observed by transmission electron microscope (TEM, TECNAI 10, Philips, Dutch). One drop of nanoparticles was placed on copper grids and negatively stained with 2% phosphotungstic acid for 30 s. Then it was dried at room temperature for about half an hour before loading on sample into equipment.

Mean Z-ave and ZP analysis:

Z-ave, PDI and ZP were determined by photon correlation spectroscopy with Zetasizer (Nano ZS90, Malvern, UK) at 25°, after appropriate dilution with ultra pure water. For Z-ave analysis, disposable polystyrene cells were used, whereas disposable plain folded capillary zeta cells were required for ZP analysis.

Encapsulation parameters:

The EE and DL capacity of CUR in SLNs were

assessed indirectly. The free CUR (nonencapsulated) and total CUR in nanoparticles suspension were determined by reverse-phase high-performance liquid chromatography (RP-HPLC, LC-15C, Shimadzu, Japan). The RP-HPLC system consisted of a reverse phase Cosmosil C18 column (4.6 mm×250 mm, 5 μm) with a UV detector set at 430 nm. The mobile phase consisted of acetonitrile: 4% glacial acetic acid (60:40, v/v) and the flow rate was 1.0 ml/min. The column temperature was 30° and the typical injection volume was 20 μl. The calibration curve was linear as $A=243433C-68007$ over the range of 0.05-40 μg/ml ($n=8$) with a correlation coefficient of $r=0.9998$ (where A =peak area and C =Cur concentration).

Free CUR was removed by ultrafiltration/centrifugation technique using Amicon Ultra-4 ultrafiltration device (molecular weight cutoff was 100 K, Millipore, USA). The sample was added into Amicon Ultra-4 ultrafiltration device after diluting suitably with purified water and centrifuged at 3500 rpm for 30 min (LC-4016 centrifuge, Anhui, China). The filtrate was removed and determined by RP-HPLC as free CUR. The sample was diluted suitably and demulsified by methanol, which was subjected to ultrasound (KQ-300B, Kunshan, China) for 5 min to make drug free from nanoparticles completely. The sample was determined by RP-HPLC as total CUR. The EE and DL of CUR in SLNs were calculated by the equations^[21] as, $EE = ((W_{total} - W_{free}) / W_{total}) \times 100\%$ and $DL = [(W_{total} - W_{free}) / (W_{total} - W_{free} + W_{lipid})] \times 100\%$, where W_{total} , W_{free} , W_{lipid} were the weight of total drug in system, weight of free drug in filtrate and weight of lipid added in system, respectively.

Differential scanning calorimetry:

Thermograms of CUR, monostearin, F68, lecithin, their physical mixture and lyophilised CUR-SLNs were recorded using DSC8222e (Mettler Toledo, Switzerland). The samples were weighed into an aluminium pan and then sealed with a pinhole-pierced cover. The heating curves of DSC were recorded at a scan rate of 10°/min from 30 to 250°.

X-ray diffraction:

The X-ray diffraction (XRD) analysis were performed on CUR, monostearin, F68, lecithin, their physical mixture and lyophilised CUR-SLNs to conduct crystalline structure of samples. The X-ray

diffractometer (D-5005, Siemens, Karlsruhe, Germany) was used. Diffractograms were performed from the initial angle $2\theta=3^\circ$ to the final angle 50° with a Cu $K\alpha$ radiation source. The obtained data were collected with a step width of 0.02° .

In vitro release studies:

The drug release of CUR-suspension and CUR-SLNs were determined using dialysis bag technique in phosphate buffer saline (pH 7.4) containing 0.5% T-80. An aliquot of 4 ml CUR-suspension and CUR-SLNs were sealed in a dialysis bag (molecular weight cutoff was 10,000 Da, Spectrum Medical Industries Inc., USA) and immersed in 200 ml of preheated release medium. The release was conducted in stirring paddle set at 100 rpm and 37°. At predetermined time intervals, 2 ml of the sample was withdrawn and replaced with the same amount of fresh release medium. The amount of Cur released from the nanoparticles was determined by RP-HPLC method as described previously for the measurement of EE. Each releasing experiment was performed in triplicate.

RESULTS AND DISCUSSION

The TEM technique was performed in order to confirm the formation and morphology of lipid nanoparticles. The measurements (fig. 1) showed that nanoparticles were prepared successfully in the shape of similar spherical structure. The diameter of nanoparticles was about 100 nm.

In order to investigate the influence of different factors on the quality of nanoparticles, single factor experiment was studied and three levels were selected in every factor. In other words, one factor of prescription was changed and the remaining factors

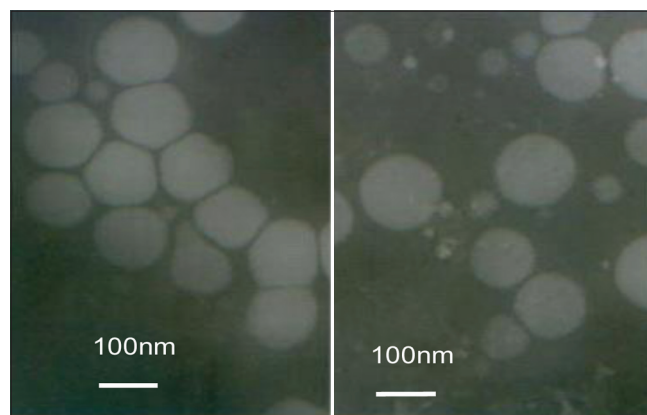


Fig. 1: Transmission electron microscopy photography of curcumin-loaded solid lipid nanoparticles.

TABLE 1: FORMULATIONS FOR THE PREPARATION OF CUR-SLNS

| Sample number | The ratio of the drug to lipid | The total amount of active agent (%) | The ratio of F68:T80 | The amount of lecithin (mg) | The time of emulsification (h) | The time of solidification (h) | Organic phase (acetone:ethanol) |
|---------------|--------------------------------|--------------------------------------|----------------------|-----------------------------|--------------------------------|--------------------------------|---------------------------------|
| 1-1 | 1:50 | 3.6 | 2:1 | 150 | 2 | 2 | 2:1 |
| 1-2 | 1:20 | 3.6 | 2:1 | 150 | 2 | 2 | 2:1 |
| 1-3 | 1:5 | 3.6 | 2:1 | 150 | 2 | 2 | 2:1 |
| 2-1 | 1:20 | 1.2 | 2:1 | 150 | 2 | 2 | 2:1 |
| 2-2 | 1:20 | 3.6 | 2:1 | 150 | 2 | 2 | 2:1 |
| 2-3 | 1:20 | 6.0 | 2:1 | 150 | 2 | 2 | 2:1 |
| 3-1 | 1:20 | 3.6 | 2:1 | 150 | 2 | 2 | 2:1 |
| 3-2 | 1:20 | 3.6 | 1:1 | 150 | 2 | 2 | 2:1 |
| 3-3 | 1:20 | 3.6 | 1:2 | 150 | 2 | 2 | 2:1 |
| 4-1 | 1:20 | 3.6 | 2:1 | 50 | 2 | 2 | 2:1 |
| 4-2 | 1:20 | 3.6 | 2:1 | 150 | 2 | 2 | 2:1 |
| 4-3 | 1:20 | 3.6 | 2:1 | 450 | 2 | 2 | 2:1 |
| 5-1 | 1:20 | 3.6 | 2:1 | 150 | 1 | 2 | 2:1 |
| 5-2 | 1:20 | 3.6 | 2:1 | 150 | 2 | 2 | 2:1 |
| 5-3 | 1:20 | 3.6 | 2:1 | 150 | 3 | 2 | 2:1 |
| 6-1 | 1:20 | 3.6 | 2:1 | 150 | 2 | 0.5 | 2:1 |
| 6-2 | 1:20 | 3.6 | 2:1 | 150 | 2 | 1 | 2:1 |
| 6-3 | 1:20 | 3.6 | 2:1 | 150 | 2 | 2 | 2:1 |
| 7-1 | 1:20 | 3.6 | 2:1 | 150 | 2 | 2 | 0:3 |
| 7-2 | 1:20 | 3.6 | 2:1 | 150 | 2 | 2 | 1:2 |
| 7-3 | 1:20 | 3.6 | 2:1 | 150 | 2 | 2 | 2:1 |

CUR-SLNS= Curcumin-loaded solid lipid nanoparticles

TABLE 2: PROPERTIES OF RESULTANT CUR-SLNS

| Sample number | EE (%) | DL (%) | Z-ave (nm) | PDI | ZP (mV) |
|---------------|------------|------------|-------------|-------------|-------------|
| 1-1 | 98.42±0.42 | 2.14±0.23 | 95.89±6.65 | 0.133±0.018 | -18.67±0.55 |
| 1-2 | 97.07±0.56 | 3.32±0.42 | 101.42±6.79 | 0.216±0.020 | -17.80±0.26 |
| 1-3 | 95.24±0.84 | 13.40±0.98 | 336.97±7.42 | 0.858±0.021 | -17.27±0.21 |
| 2-1 | 97.54±0.58 | 3.30±0.21 | 295.20±7.19 | 0.858±0.146 | -17.10±0.75 |
| 2-2 | 97.07±0.56 | 3.32±0.42 | 101.42±6.80 | 0.216±0.020 | -17.80±0.26 |
| 2-3 | 96.96±0.65 | 3.37±0.18 | 87.16±6.78 | 0.229±0.020 | -18.90±0.55 |
| 3-1 | 97.07±0.56 | 3.32±0.42 | 101.42±6.80 | 0.216±0.020 | -17.80±0.26 |
| 3-2 | 97.42±0.74 | 4.18±0.36 | 95.57±6.17 | 0.193±0.035 | -19.60±0.26 |
| 3-3 | 97.42±0.58 | 4.32±0.28 | 92.97±6.00 | 0.182±0.024 | -16.10±0.53 |
| 4-1 | 97.81±0.63 | 3.83±0.36 | 70.67±3.30 | 0.322±0.035 | -18.37±0.23 |
| 4-2 | 97.07±0.56 | 3.32±0.42 | 101.42±6.80 | 0.216±0.020 | -17.80±0.26 |
| 4-3 | 97.75±0.78 | 3.58±0.18 | 113.83±6.42 | 0.259±0.019 | -19.30±0.20 |
| 5-1 | 97.06±0.35 | 4.13±0.17 | 109.67±5.69 | 0.245±0.020 | -10.07±0.46 |
| 5-2 | 97.07±0.56 | 3.32±0.42 | 101.42±6.80 | 0.216±0.020 | -17.80±0.27 |
| 5-3 | 97.62±0.55 | 3.65±0.29 | 102.17±6.38 | 0.208±0.008 | -19.13±0.19 |
| 6-1 | 97.29±0.43 | 3.78±0.47 | 99.82±6.13 | 0.232±0.009 | -16.43±0.15 |
| 6-2 | 97.19±0.72 | 3.61±0.59 | 90.68±6.23 | 0.196±0.013 | -21.4±1.04 |
| 6-3 | 97.07±0.56 | 3.32±0.42 | 101.42±6.80 | 0.216±0.020 | -17.80±0.27 |
| 7-1 | 94.24±0.39 | 3.02±0.38 | 86.32±3.43 | 0.143±0.023 | -19.77±1.04 |
| 7-2 | 95.67±0.47 | 3.22±0.37 | 85.54±5.09 | 0.145±0.012 | -19.17±0.76 |
| 7-3 | 97.07±0.56 | 3.32±0.42 | 101.42±6.80 | 0.216±0.020 | -17.80±0.27 |

EE=encapsulation efficiency, DL=drug loading, Z-ave=particles size, PDI=polydispersity index, ZP=zeta potential, SD=standard deviation. Data represented as mean±SD (n=3), CUR-SLNS= Curcumin-loaded solid lipid nanoparticles

were unchanged in each group of experiments. Z-ave, PDI, ZP, EE and DL capacity were as evaluation criteria. Photon correlation spectroscopy was applied to obtain accurate data on nanoparticles and Z-ave,

PDI and ZP were obtained. EE and DL capacity were determined by RP-HPLC. The specific composition and results of formulations are shown in Tables 1 and 2.

Table 2 shows that EE and DL capacity were ranged from 94.24 to 98.42% and from 2.14 to 13.40%, respectively. The mean Z-ave was approximately 100 nm with a narrow PDI for all developed formulations, which were in agreement with TEM results. ZP values was in the range -10.07 mV to -21.4 mV providing good physical stability to the formulations within a period of time.

As indicated by the sample 1 in Table 2, the ratio of the drug to lipid and the organic phase had a greater impact on EE and DL capacity. The DL capacity was improved significantly by increasing ratio of the drug to lipid; however, EE decreased thereon. The organic phase with 1 ml ethanol and 2 ml acetone had higher EE and DL capacity. From the sample nos. 1, 2, 4 and 7 in Table 2, we could see Z-ave and PDI were closely related to the ratio of the drug to lipid, the total amount of active agent, the amount of lecithin and the organic phase. Z-ave and PDI were increased with more drugs. Higher proportion of active agent showed smaller Z-ave and narrow PDI. It may be because the nanoemulsion was emulsified completely with more active agent. The ZP of all developed formulations revealed that different formulations had no significant difference except sample 5-1 with low absolute ZP. The result of sample 5-1 implied nanoparticles emulsion had poor stability, which was attributed to the small amount of lecithin and short emulsification time.

Based on the results of a single factor analysis, ratio of the drug to lipid, total amount of active agent, amount of lecithin, and organic phase were selected as main factors affecting the quality of nanoparticles

and three levels were set in each factor according to orthogonal test L9 (3^4) table. The evaluation criterion was the same as the single factor test. The Z-ave, PDI, ZP, EE, and DL capacity of the optimised formulation were 99.99 nm, 0.158, -19.9 mV, 97.86% and 4.35%, respectively.

DSC and XRD were applied to understand polymorphic state and structure of nanoparticles. From the DSC curves (fig. 2), the single melting endothermic peak of CUR was observed at 183.2° corresponding to its melting point. The melting endothermic peaks of CUR and excipient were visible in the physical mixture (fig. 2). However, the melting endothermic peaks of lyophilised CUR-SLNs appeared at 50.5° and 166.8° with the disappearance of melting endothermic peak of CUR, indicating CUR was essentially encapsulated into the lipid with amorphous state (fig. 2). The diffraction pattern exhibited CUR (fig. 3a) had two sharp peaks at $2\theta=8.78^\circ$ and 17.16° , and some peaks of lower intensity. Main reflections of monostearin (fig. 3b) at $2\theta=19.85^\circ$, 20.62° and F68 (fig. 3c) at $2\theta=19.08^\circ$, 23.26° were also found. These results indicated the crystalline nature of CUR, monostearin and F68. The diffraction characterised peaks appeared in the physical mixture (fig. 3e). In contrast, the absence of these characteristics reflections in lyophilised CUR-SLNs (fig. 3f) demonstrated the total solubilisation of drug within the lipid phase. XRD data were in good agreement with the results depicted by DSC measurement.

The release profile of CUR-suspension and CUR-SLNs *in vitro* were studied. Because of

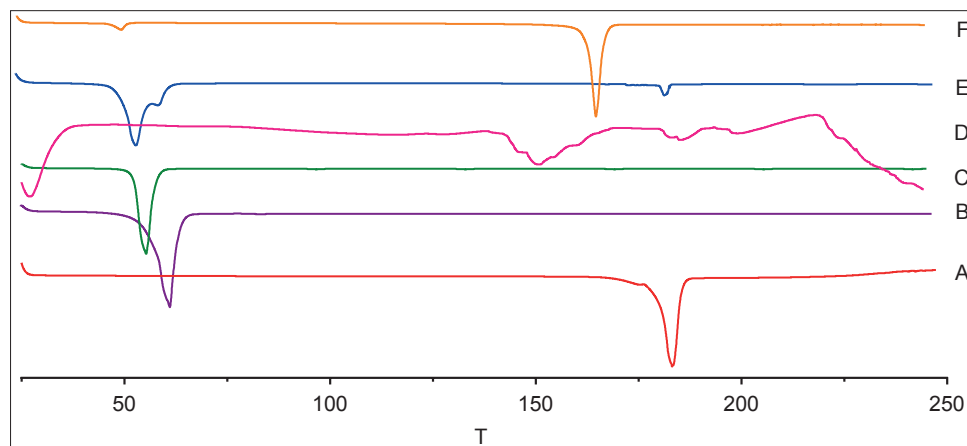


Fig. 2: Differential scanning calorimetry thermograms. Curcumin (A), monostearin (B), F68 (C), lecithin (D), physical mixture (E), and lyophilised CUR-SLNs powders (F), T=temperature (°).

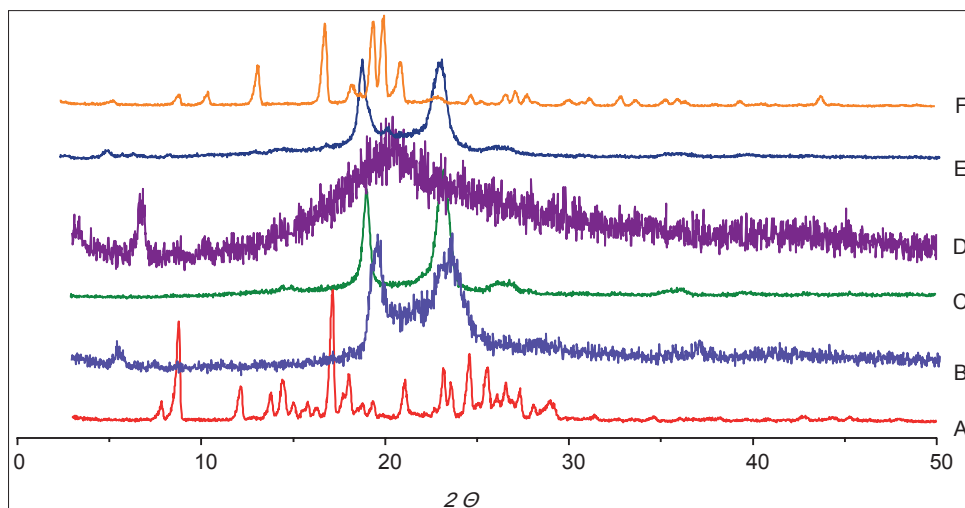


Fig. 3: The X-ray diffraction patterns. Curcumin (A), monostearin (B), F68 (C), lecithin (D), physical mixture (E) and lyophilised CUR-SLNs powders (F).

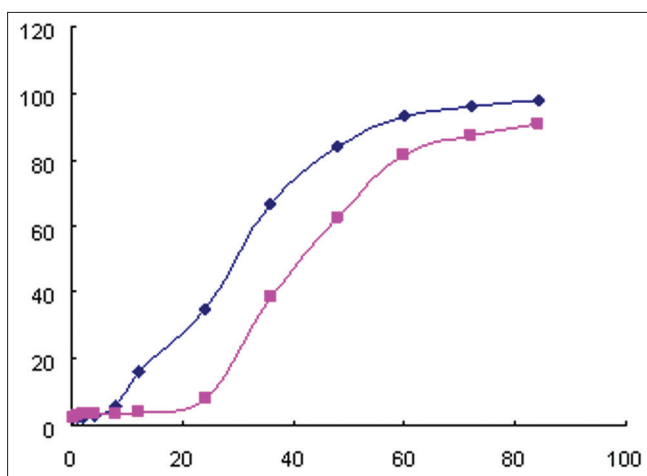


Fig. 4: *In vitro* drug release profiles of curcumin and CUR-SLNs. —◆— represents the release profile of curcumin; —■— represents the release profile of CUR-SLNs, $n=3$.

the low solubility of CUR in water, phosphate buffer saline (pH 7.4) containing 0.5% T-80 was selected as release medium. As shown in fig. 4, the CUR-suspension showed quick release with a cumulative release 35.05% at 24 h and 97.47% at 84 h. The release data were fitted to Niebergull model with equation as $(1-Q\%)^{1/2} = -0.0113t + 1.0178$. However, the CUR-SLNs was released slowly at initial, only 7.8% at 24 h. The release rate increased after 24 h and gradually level off. The release kinetics of CUR-SLNs was fitted to Niebergull equation, described as $(1-Q\%)^{1/2} = -0.0089t + 1.0415$. The release profile was explained that some drug existed in the exterior lipid layer of the nanoparticles. The high drug concentration near the surfactant-lipid boundary resulted from the diffusion of CUR during

nanoparticles. A sustained release of CUR was because the shear stress of agitation demolished the surfactant layer on CUR-SLNs. Therefore, the decomposition of integrated structure of the lipid core controlled the release rate of CUR^[22,23].

CUR-SLNs were prepared successfully with lipid as the carrier by emulsion-evaporation and low temperature-solidification technique. The formulations were optimised by the single factor analysis and orthogonal design. The obtained SLNs was suspension of nanosized homogeneous nanoparticles with high EE and DL capacity. ZP values results suggested that prepared nanoparticles provided good physical stability within a period of time. The results of DSC and XRD analysis demonstrated drug had been encapsulated or absorbed by lipid carriers. The release experiments *in vitro* exhibited CUR-SLNs can delay drug release comparing with CUR-suspension. Therefore, SLNs would provide highly desirable physicochemical characteristics as a new type of colloidal drug delivery systems of lipophilic drug as CUR. The profile of tissue distribution and pharmacokinetics *in vivo* are being researched in our present experiments, which will be reported in the near future.

REFERENCES

1. Müller RH, Shegokar R, Keck CM. 20 years of lipid nanoparticles (SLN and NLC): Present state of development and industrial applications. *Curr Drug Discov Technol* 2011;8:207-27.
2. Nair HB, Sung B, Yadav VR, Kannappan R, Chaturvedi MM, Aggarwal BB. Delivery of antiinflammatory nutraceuticals by nanoparticles for the prevention and treatment of cancer. *Biochem*

- Pharmacol 2010;80:1833-43.
3. Rai B, Kaur J, Catalina M. Antioxidation actions of curcumin in two forms of bed rest: Oxidative stress serum and salivary markers. *Asian Pac J Trop Med* 2010;3:651-4.
 4. Rai D, Singh JK, Roy N, Panda D. Curcumin inhibits FtsZ assembly: An attractive mechanism for its antibacterial activity. *Biochem J* 2008;410:147-55.
 5. Babaei E, Sadeghizadeh M, Hassan ZM, Feizi MA, Najafi F, Hashemi SM. Dendrosomal curcumin significantly suppresses cancer cell proliferation *in vitro* and *in vivo*. *Int Immunopharmacol* 2012;12:226-34.
 6. Aggarwal BB, Kumar A, Bharti AC. Anticancer potential of curcumin: Preclinical and clinical studies. *Anticancer Res* 2003;23:363-98.
 7. Peschel D, Koerting R, Nass N. Curcumin induces changes in expression of genes involved in cholesterol homeostasis. *J Nutr Biochem* 2007;18:113-9.
 8. Deeb D, Jiang H, Gao X, Hafner MS, Wong H, Divine G, *et al.* Curcumin sensitizes prostate cancer cells to tumor necrosis factor-related apoptosis-inducing ligand/Apo2L by inhibiting nuclear factor-kappaB through suppression of I κ B α phosphorylation. *Mol Cancer Ther* 2004;3:803-12.
 9. Duvoix A, Blasius R, Delhalle S, Schneckeburger M, Morceau F, Henry E, *et al.* Chemopreventive and therapeutic effects of curcumin. *Cancer Lett* 2005;223:181-90.
 10. Perkins S, Verschoyle RD, Hill K, Parveen I, Threadgill MD, Sharma RA, *et al.* Chemopreventive efficacy and pharmacokinetics of curcumin in the min/+ mouse, a model of familial adenomatous polyposis. *Cancer Epidemiol Biomarkers Prev* 2002;11:535-40.
 11. Rahman I, Adcock IM. Oxidative stress and redox regulation of lung inflammation in COPD. *Eur Respir J* 2006;28:219-42.
 12. Fiala M, Liu PT, Espinosa-Jeffrey A, Rosenthal MJ, Bernard G, Ringman JM, *et al.* Innate immunity and transcription of MGAT-III and Toll-like receptors in Alzheimer's disease patients are improved by bisdemethoxycurcumin. *Proc Natl Acad Sci USA* 2007;104:12849-54.
 13. Wei SM, Yan ZZ, Zhou J. Curcumin attenuates ischemia-reperfusion injury in rat testis. *Fertil Steril* 2009;91:271-7.
 14. Murakami A, Ohigashi H. Targeting NOX, INOS and COX-2 in inflammatory cells: Chemoprevention using food phytochemicals. *Int J Cancer* 2007;121:2357-63.
 15. Mulik RS, Mönkkönen J, Juvonen RO, Mahadik KR, Paradkar AR. Transferrin mediated solid lipid nanoparticles containing curcumin: Enhanced *in vitro* anticancer activity by induction of apoptosis. *Int J Pharm* 2010;398:190-203.
 16. Tønnesen HH, Karlsen J, van Henegouwen GB. Studies on curcumin and curcuminoids. VIII. Photochemical stability of curcumin. *Z Lebensm Unters Forsch* 1986;183:116-22.
 17. Wang YJ, Pan MH, Cheng AL, Lin LI, Ho YS, Hsieh CY, *et al.* Stability of curcumin in buffer solutions and characterization of its degradation products. *J Pharm Biomed Anal* 1997;15:1867-76.
 18. Chirio D, Gallarate M, Peira E, Battaglia L, Serpe L, Trotta M. Formulation of curcumin-loaded solid lipid nanoparticles produced by fatty acids coacervation technique. *J Microencapsul* 2011;28:537-48.
 19. Harde H, Das M, Jain S. Solid lipid nanoparticles: An oral bioavailability enhancer vehicle. *Expert Opin Drug Deliv* 2011;8:1407-24.
 20. Jia LJ, Zhang DR, Li ZY, Feng FF, Wang YC, Dai WT, *et al.* Preparation and characterization of silybin-loaded nanostructured lipid carriers. *Drug Deliv* 2010;17:11-8.
 21. Dai W, Zhang D, Duan C, Jia L, Wang Y, Feng F, *et al.* Preparation and characteristics of oridonin-loaded nanostructured lipid carriers as a controlled-release delivery system. *J Microencapsul* 2010;27:234-41.
 22. Kuo YC, Chung JF. Physicochemical properties of nevirapine-loaded solid lipid nanoparticles and nanostructured lipid carriers. *Colloids Surf B Biointerfaces* 2011;83:299-306.
 23. Kuo YC, Chen HH. Entrapment and release of saquinavir using novel cationic solid lipid nanoparticles. *Int J Pharm* 2009;365:206-13.

Accepted 23 February 2013

Revised 17 February 2013

Received 23 August 2012

Indian J Pharm Sci 2013;75(2):178-184